

A deterministic spectral method for solving the Boltzmann equation for one-dimensional flows

Chatcharuangsawit^{a,*}, Yurii N. Grigoriev^b, Sergey V. Meleshko^a

^a School of Mathematics, Suranaree University of Technology, Nakorn Ratchasima 30000, Thailand

^b Institute of Computational Technologies, Novosibirsk, Russia

* Corresponding author, e-mail: chat@math.sut.ac.th

Received 30 Apr 2008

Accepted 5 Jan 2009

ABSTRACT: A new deterministic numerical method for solving the kinetic Boltzmann equation for Maxwellian molecules with cylindrical symmetry in velocity space is developed. Using the splitting method with respect to physical processes, the Boltzmann equation is decomposed into the space-homogeneous Boltzmann equation and the transport equation. The transport equation is solved by either Lax-Wendroff or upwind schemes. For Maxwell's model, the space-homogeneous Boltzmann equation is simplified by taking the Fourier transform with respect to velocity. Because of the cylindrical symmetry in velocity space, the three-dimensional Fourier transform is equivalent to a one-dimensional Fourier transform and a Hankel transform. An exponential grid in velocity space allows the application a fast Fourier transform algorithm to compute the Hankel transform. The space homogeneous Boltzmann equation in Fourier space is solved by the Runge-Kutta scheme. The new method is applied to solving the heat transfer problem between parallel plates.

KEYWORDS: kinetic theory, Maxwellian model, Fourier transform, Hankel transform, heat transfer problem

INTRODUCTION

The classical Boltzmann equation is the main mathematical tool of the kinetic theory of gases^{1,2}. On the one hand, this equation serves for the axiomatic construction of continuous medium models such as the gas dynamics, Navier-Stokes, and Barnette equations. At the same time, asymptotic solutions of the Boltzmann equation enable one to obtain the explicit form of transport coefficients such as viscosity, thermal conductivity, and diffusivity. On the other hand, these equations are used for describing rarefied gas flows. Rarefaction is quantified by the Knudsen number $\text{Kn} = \lambda/L$, where λ is the mean free path of the molecules and L is the characteristic scale of the flow. The application of kinetic equations is confined to systems for which $0.1 < \text{Kn} < 10.0^1$. These flows are realized in a wide range of scales from galactic to microscopic. Examples include the so-called jets and turbulence piles in the far reaches of the cosmos, flows over spacecraft during their descent through the upper atmospheres of planets, flows in vacuum chemical reactors, overflowing aerosol particles of micron scale in problems of ecology, flows in micro-electrical machine systems, and scattering of ultrasonic waves.

The Boltzmann equation is an integro-differential equation. Its characteristic feature is the presence of a

multi-dimensional nonlinear operator, called the collision integral, and its resulting complexity excludes the possibility of obtaining exact solutions and generates formidable difficulties for the application of numerical methods.

Two distinct groups of numerical methods for solving the Boltzmann equation have been developed (a general review of the methods and relations between them can be found in Ref. 3). The first group combines methods of direct modelling type such as the direct simulation Monte-Carlo (DSMC) method⁴. The rapid expansion of these methods in the last three decades was motivated by the development of space aerodynamics. They are based on the stochastic nature of the elementary processes of gas molecule kinetics. From the computational point of view, the principal feature of these methods consists of using Monte-Carlo procedures for modelling molecular scattering described by the collision integral.

The second group comprises regular (deterministic) methods of direct numerical solution of the Boltzmann equation³. Such methods are exclusively based on well-known algorithms of numerical analysis such as spline interpolation, finite-difference or finite-volume schemes, and quadrature formulas.

The DSMC methods have indisputable priority in applied problems of rarefied gas dynamics where one

needs to compute fluxes of mass, impulse, and energy on surfaces over which fluid is flowing. However, regular methods allow, in principle, the finding of solutions of the Boltzmann equation at a wide range of molecular energies which are beyond the DSMC method possibilities. This is very important in computing threshold processes in shock waves, such as those involving chemical reactions with a large activation energy. Moreover, good deterministic methods give an opportunity to obtain very precise standard numerical solutions. They are necessary, in particular, for validation of new modifications of DSMC methods which often deviate from strict adherence to the Boltzmann equation.

A scheme of a deterministic spectral method for the Boltzmann equation with Maxwellian molecules has been proposed⁵. The algorithm is based on the splitting method with respect to physical processes with stages of space-free molecular transport and space-homogeneous collision relaxation. The more laborious stage of relaxation is based on the Fourier transform, which makes the algorithm optimal with respect to the amount of computation. The number of computations is estimated as $O(N \log_2 N)$, where N is the number of elements in the computing array. Such optimal computational cost is determined by using an exact Fourier representation of the collision integral. This representation is a two-fold integral over angle scattering variables which substantially reduces the volume of computations. Such transformation is only possible for a collision integral with Maxwellian molecules⁵. Various deterministic algorithms for the Boltzmann equation with other molecular models have been proposed^{3,6-8}. However, the computational costs of these algorithms is considerably higher than the algorithm presented in this paper.

In this paper a regular numerical method of direct integration for the case of one-dimensional flows is developed. Such flows have axial symmetry in molecular velocity space. Despite obvious restrictions there are a great number of problems of this type. Among them are classical problems of gas kinetic theory such as heat and mass transfer (recondensation) between parallel plates, or the problem of a plane shock wave structure. Also, there is a set of problems of practical interest such as the investigation of evaporation and nucleation of spherical drops, which are active centres in the formation of smog and fog as well in the process of condensation in different technical plants. Other examples include energetic particles escaping from spherical planet atmospheres, absorption and condensation processes on cylindrical jets, and burnout of cylindrical cathodes of electron devices.

In the present paper, a new deterministic method is described. Selection of numerical procedures of transport and relaxation stages are presented and discussed. Comparison of test results with exact solutions is given. As a first example of the application of the developed method, the problem of heat transfer between parallel plates is solved.

THE BOLTZMANN EQUATION AND STATEMENT OF PROBLEM

The Boltzmann equation describes the evolution of rarefied gas in terms of a molecular distribution function. Without external forces, the Boltzmann equation of a monatomic gas can be written as^{1,2}

$$\frac{\partial f}{\partial t} + \mathbf{v} \cdot \nabla_{\mathbf{x}} f = Q(f, f). \quad (1)$$

Here $\mathbf{x} \in R^3(\mathbf{x})$ is the space coordinate, $\mathbf{v} \in R^3(\mathbf{v})$ is the molecular velocity, and $f = f(\mathbf{x}, \mathbf{v}, t)$ is the distribution function, which defines the mean molecular density at time t in the differential volume $d\mathbf{x} d\mathbf{v}$ near a point (\mathbf{x}, \mathbf{v}) of six-dimensional phase space $R^3(\mathbf{x}) \times R^3(\mathbf{v})$. If the distribution function $f = f(\mathbf{v}, t)$ is independent of the variable \mathbf{x} , one deals with the space-homogeneous Boltzmann equation. The term $Q(f, f)$ is called the collision operator and is defined by

$$Q(f, f)(\mathbf{x}, \mathbf{v}, t) = \int_{R^3} \int_{S^2} B(w, \theta) [f' f'_1 - f f_1] d\mathbf{n} d\mathbf{v}_1, \quad (2)$$

where $f' = f(\mathbf{x}, \mathbf{v}', t)$, $f'_1 = f(\mathbf{x}, \mathbf{v}'_1, t)$, $f = f(\mathbf{x}, \mathbf{v}, t)$, $f_1 = f(\mathbf{x}, \mathbf{v}_1, t)$, \mathbf{v} and \mathbf{v}_1 are the pre-collision velocities of a colliding pair of molecules, \mathbf{v}' and \mathbf{v}'_1 are the corresponding velocities after collision, and $\mathbf{w} = \mathbf{v} - \mathbf{v}_1$ is the relative velocity of the two molecules before collision. The parameter θ is the scattering angle between \mathbf{w} and $\mathbf{w}' = \mathbf{v}' - \mathbf{v}'_1$, $d\mathbf{n}$ is the differential surface element on the unit sphere $S^2 = \{\mathbf{n} \in R^3, |\mathbf{n}| = 1\}$. The velocities of colliding molecules satisfy the microscopic momentum and energy conservation laws

$$\mathbf{v}' + \mathbf{v}'_1 = \mathbf{v} + \mathbf{v}_1, \quad |\mathbf{v}'|^2 + |\mathbf{v}'_1|^2 = |\mathbf{v}|^2 + |\mathbf{v}_1|^2. \quad (3)$$

The post-collision velocities are defined by

$$\begin{aligned} \mathbf{v}' &= \frac{1}{2} (\mathbf{v} + \mathbf{v}_1 + |\mathbf{v} - \mathbf{v}_1| \mathbf{n}), \\ \mathbf{v}'_1 &= \frac{1}{2} (\mathbf{v} + \mathbf{v}_1 - |\mathbf{v} - \mathbf{v}_1| \mathbf{n}). \end{aligned}$$

The kernel B is a scattering function which has the form

$$B(w, \theta) = w\sigma(w, \cos\theta), \quad (4)$$

where the function $\sigma : R^+ \times [-1, 1] \rightarrow R^+$ is a differential cross-section. The scattering function B characterizes details of the binary interactions depending on the physical properties of the gas molecules.

Two special cases of the scattering function B are used in the paper. The main model is that of Maxwellian molecules with the scattering function

$$B(w, \theta) = g(\cos\theta), \quad (5)$$

which does not depend on the modulus of the relative velocity w . The other is the model of so-called “hard sphere” molecules with the scattering function

$$B(w, \theta) = w \frac{d^2}{4}, \quad (6)$$

where d is the molecular diameter.

All macroscopic properties of a gas can be defined in terms of f . In particular, the density, mean bulk velocity, and temperature of the gas are given respectively by

$$n(\mathbf{x}, t) = \int_{R^3(\mathbf{v})} f(\mathbf{x}, \mathbf{v}, t) d\mathbf{v}, \quad (7)$$

$$\mathbf{u}(\mathbf{x}, t) = \frac{1}{n(\mathbf{x}, t)} \int_{R^3(\mathbf{v})} \mathbf{v} f(\mathbf{v}) d\mathbf{v}, \quad (8)$$

$$T(\mathbf{x}, t) = \frac{1}{3n(\mathbf{x}, t)R} \int_{R^3(\mathbf{v})} |\mathbf{v} - \mathbf{u}|^2 f(\mathbf{v}) d\mathbf{v}, \quad (9)$$

where R is the gas constant.

The Boltzmann collision operator has the following fundamental properties of conserving mass, momentum, and energy:

$$\int_{R^3(\mathbf{v})} Q(f, f) d\mathbf{v} = 0, \quad (10)$$

$$\int_{R^3(\mathbf{v})} \mathbf{v} Q(f, f) d\mathbf{v} = 0, \quad (11)$$

$$\int_{R^3(\mathbf{v})} |\mathbf{v}|^2 Q(f, f) d\mathbf{v} = 0. \quad (12)$$

For the space homogeneous Boltzmann equation these properties give us conservation of the gas dynamic parameters $n(t)$, $\mathbf{u}(t)$ and $T(t)$ during the time evolution of the distribution function $f(\mathbf{v}, t)$ from any initial distribution $f_0(\mathbf{v})$.

Consider the Cauchy problem for the space homogeneous Boltzmann equation

$$\begin{aligned} \frac{\partial f(\mathbf{x}, \mathbf{v}, t)}{\partial t} &= Q(f, f)(\mathbf{x}, \mathbf{v}, t), \\ f(\mathbf{x}, \mathbf{v}, 0) &= f_0(\mathbf{x}, \mathbf{v}). \end{aligned} \quad (13)$$

The Fourier transform $\varphi(\mathbf{x}, \mathbf{k}, t)$ of the distribution function $f(\mathbf{x}, \mathbf{v}, t)$ in velocity space is defined as

$$\varphi(\mathbf{x}, \mathbf{k}, t) = \int_{R^3(\mathbf{v})} e^{-i2\pi(\mathbf{v} \cdot \mathbf{k})} f(\mathbf{x}, \mathbf{v}, t) d\mathbf{v}. \quad (14)$$

Using the Fourier transform (14), the problem (13) for Maxwellian molecules can be transformed to the form⁹

$$\begin{aligned} &\frac{\partial \varphi(\mathbf{x}, \mathbf{k}, t)}{\partial t} \\ &= \int_{S^2} \left[\varphi\left(\mathbf{x}, \frac{\mathbf{k} + k\mathbf{n}}{2}, t\right) \varphi\left(\mathbf{x}, \frac{\mathbf{k} - k\mathbf{n}}{2}, t\right) \right. \\ &\quad \left. - \varphi(\mathbf{x}, \mathbf{k}, t) \varphi(\mathbf{x}, \mathbf{0}, t) \right] g(\cos\theta) d\mathbf{n}, \end{aligned} \quad (15)$$

$$\varphi(\mathbf{x}, \mathbf{k}, 0) = \int_{R^3(\mathbf{v})} f(\mathbf{x}, \mathbf{v}, 0) e^{-i2\pi(\mathbf{v} \cdot \mathbf{k})} d\mathbf{v}.$$

If we assume that the distribution function possesses cylindrical symmetry with respect to the velocity variable \mathbf{v} , i.e., $f(\mathbf{x}, \mathbf{v}, t) = f(\mathbf{x}, v_x, v_r, t)$ where $\mathbf{v} = (v_x, v_y, v_z)$ and $v_r^2 = v_y^2 + v_z^2$, then the Fourier transform (14) of $f(\mathbf{x}, \mathbf{v}, t)$ also possesses cylindrical symmetry¹⁰ and

$$\begin{aligned} \varphi(k_x, k_r, t) &= 2\pi \int_{-\infty}^{\infty} e^{-i2\pi k_x v_x} \int_0^{\infty} J_0(2\pi k_r v_r) \\ &\quad \times v_r f(v_x, v_r) dv_r dv_x, \end{aligned} \quad (16)$$

$$\begin{aligned} f(v_x, v_r) &= 2\pi \int_{-\infty}^{\infty} e^{i2\pi k_x v_x} \int_0^{\infty} J_0(2\pi k_r v_r) \\ &\quad \times v_r \varphi(k_x, k_r) dk_r dk_x. \end{aligned} \quad (17)$$

The inner integrals in these formulas are the Hankel transforms with respect to the corresponding variables. Because the variables \mathbf{x} and t are not invoked while taking the Fourier transform in velocity space, for the sake of simplicity they are omitted from now on.

Let us consider in (15) the Fourier transform (14) of the collision integral $Q(f, f)$ which will be denoted by $\hat{Q}(\varphi, \varphi)$. Since $\varphi(\mathbf{k})$ possesses cylindrical symmetry, one can write

$$\varphi\left(\frac{\mathbf{k} \pm k\mathbf{n}}{2}\right) = \varphi\left(\frac{k_x + kn_x}{2}, \left|\frac{\mathbf{k}_r \pm k\mathbf{n}_r}{2}\right|\right) \quad (18)$$

where

$$\left|\frac{\mathbf{k}_r \pm k\mathbf{n}_r}{2}\right| = \frac{1}{2} \sqrt{k_r^2 + k^2|\mathbf{n}_r|^2 \pm 2k\mathbf{k}_r \cdot \mathbf{n}_r}$$

where $\mathbf{k}_r = k_y \mathbf{e}_y + k_z \mathbf{e}_z$, $\mathbf{n}_r = n_y \mathbf{e}_y + n_z \mathbf{e}_z$.

For simplicity, the case of Maxwellian molecules with isotropic scattering $g(\cos \theta) = \sigma_0/4\pi$ is considered further. After some calculations it can be shown that

$$\hat{Q}(\varphi, \varphi) = \frac{\sigma_0}{\pi} \int_0^{\frac{\pi}{2}} \int_0^1 [\varphi_{(+,+)} \varphi_{(-,-)} + \varphi_{(+,-)} \varphi_{(-,+)} - 2\varphi(k_x, k_r) \varphi(\mathbf{0})] d\mu d\alpha, \quad (19)$$

where

$$\varphi_{(\circledast, \circledot)} \equiv \varphi \left(\frac{k_x \circledast k \mu}{2}, \frac{1}{2} \sqrt{k_r^2 + k^2(1 - \mu^2) \odot 2k_r k \sqrt{1 - \mu^2} \cos \alpha} \right),$$

in which \circledast and \circledot can be either $+$ or $-$.

The algorithm for solving the Boltzmann equation developed in this paper assumes that the distribution function depends on one space coordinate x and that the mean gas velocity \mathbf{u} is directed along this coordinate. In this case the distribution function and its Fourier transform possess the cylindrical symmetry considered above. Boundaries can be composed of infinite parallel plates, coaxial circular cylinders, or concentric spheres. In all these cases the problem can be stated on finite or semi-infinite intervals. In the first case the infinite interval $x \in (-\infty, \infty)$ can also be considered. In cylindrical and spherical geometries, the inner boundary can be replaced by a δ -source or drain.

In this paper the study is restricted to the case of plane geometry. For definiteness let us consider a gas flow between two parallel infinite flat plates which are separated by a distance L (Fig. 1). In this case the distribution function $f(\mathbf{x}, \mathbf{v}, t)$ only depends on the variables x, v_x, v_r , and t , and the classical initial-

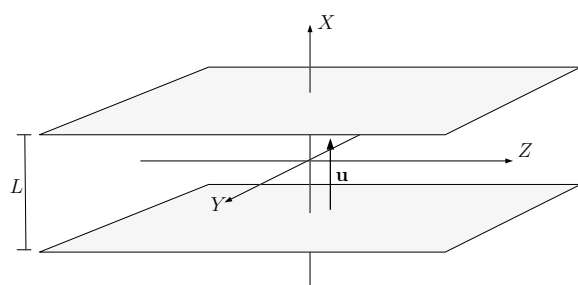


Fig. 1 Flow between two flat plates.

boundary problem has the form¹

$$\frac{\partial f}{\partial t} + v_x \frac{\partial f}{\partial x} = \frac{\sigma_0}{4\pi} \int_{R^3(\mathbf{v})} \int_{S^2} [f(\mathbf{v}') f(\mathbf{v}'_1) - f(\mathbf{v}) f(\mathbf{v}_1)] d\mathbf{n} d\mathbf{v}_1, \quad (20)$$

$$\begin{aligned} f(x, v_x, v_r, 0) &= f^0(x, v_x, v_r), \\ f(L/2, v_x, v_r) &= n_+ \left(\frac{2\pi k T_+}{m} \right)^{-\frac{3}{2}} \\ &\times e^{-m(v_x^2 + v_r^2)/2kT_+}, \quad (v_x < 0), \\ f(-L/2, v_x, v_r) &= n_- \left(\frac{2\pi k T_-}{m} \right)^{-\frac{3}{2}} \\ &\times e^{-m(v_x^2 + v_r^2)/2kT_-}, \quad (v_x > 0). \end{aligned} \quad (21)$$

Here k is the Boltzmann constant, m is the mass of the molecules, and n_+, T_+ and n_-, T_- are, the number densities and temperatures at the top and bottom plates, respectively. Their values depend on the physical conditions on the plates such as sorption, evaporation, impenetrability, momentum and energy accommodation. For curvilinear boundaries the differential operator of the Boltzmann equation is more complicated than in (20) and contains additional terms¹.

Characteristic values for the dimensionless form of the initial-boundary problem, (20) and (21), are chosen as follows: $f_0 = \bar{n}(kT_-/m)^{-3/2}$, $t_0 = L(kT_-/m)^{-1/2}$, $v_0 = L/t_0 = (kT_-/m)^{1/2}$, $x_0 = L$. Here \bar{n} is the mean number density of a gas in the segment $[-L/2, L/2]$, and is defined as

$$\bar{n} = \frac{1}{L} \int_{-L/2}^{L/2} n(x) dx,$$

where $n(x)$ is the local number density (7).

The dimensionless variables are related to the original variables by $f(t, \mathbf{x}, \mathbf{v}) = f_0 \tilde{f}(\tilde{t}, \tilde{\mathbf{x}}, \tilde{\mathbf{v}})$, $t = t_0 \tilde{t}$, $v = v_0 \tilde{v}$, $x = x_0 \tilde{x}$, $T = T_- \tilde{T}$. Using these relations, (20) and (21) become

$$\begin{aligned} \frac{\partial \tilde{f}}{\partial \tilde{t}} + \tilde{v}_x \frac{\partial \tilde{f}}{\partial \tilde{x}} &= \frac{1}{4\pi K n} \int_{R^3(\tilde{\mathbf{v}})} \int_{S^2} [f(\tilde{\mathbf{v}}') f(\tilde{\mathbf{v}}'_1) \\ &- f(\tilde{\mathbf{v}}) f(\tilde{\mathbf{v}}_1)] d\tilde{\mathbf{n}} d\tilde{\mathbf{v}}_1, \end{aligned} \quad (22)$$

$$\tilde{f}(\tilde{x}, \tilde{v}_x, \tilde{v}_r, 0) = \tilde{f}^0(\tilde{x}, \tilde{v}_x, \tilde{v}_r),$$

$$\begin{aligned} \tilde{f}\left(\frac{1}{2}, \tilde{v}_x, \tilde{v}_r\right) &= \tilde{n}_+ \left(2\pi \tilde{T}_+ \right)^{-\frac{3}{2}} e^{-\frac{(\tilde{v}_x^2 + \tilde{v}_r^2)}{2\tilde{T}_+}}, \quad (\tilde{v}_x < 0), \\ \tilde{f}\left(-\frac{1}{2}, \tilde{v}_x, \tilde{v}_r\right) &= \tilde{n}_- (2\pi)^{-\frac{3}{2}} e^{-\frac{(\tilde{v}_x^2 + \tilde{v}_r^2)}{2}}, \quad (\tilde{v}_x > 0), \end{aligned} \quad (23)$$

where $\text{Kn} = 1/(\sigma_0 f_0 t_0 v_0^3)$ is the Knudsen number. From now on we drop the tildes.

SPLITTING SCHEME AND NUMERICAL PROCEDURES

For solving the problem formulated above, the splitting method with respect to physical processes is used. The solution of the initial-boundary problem (22), (23) in each time interval $[t_n, t_n + \tau]$ is obtained by successively solving the initial-boundary problem of the transport equation

$$\hat{f}_t = -A\hat{f}, \quad \hat{f}(x, v_x, v_r, t_n) = f(x, v_x, v_r, t), \quad (24)$$

and the Cauchy problem of the space-homogeneous Boltzmann equation

$$f_t = Q(f, f), \quad f(x, v_x, v_r, t_n) = \hat{f}(x, v_x, v_r, t_n + \tau), \quad (25)$$

where A is the differential operator on the left-hand side of the Boltzmann equation (22) with boundary conditions (23).

For computing $\hat{f}(x, v, t_n + \tau)$ the Fourier transform of the space-homogeneous Boltzmann equation (15) is used:

$$\varphi_t = \hat{Q}(\varphi, \varphi). \quad (26)$$

The use of the fast Fourier transform (FFT) procedure¹¹ at the stage of collision relaxation (25) results in an algorithm requiring $O(N \log_2 N)$ operations⁵, where N is the number of grid points in the calculation domain.

During numerical integration of (24) it is necessary to conserve positive definiteness of the distribution function $\hat{f}(x, v, t_n + \tau)$ which is related to the monotonicity property of the finite-difference scheme. The upwind scheme possesses such a property¹², but it is first order in t and x , and because of the scheme viscosity it can bring in significant errors. Therefore the following recommendations¹³ were used. If sufficient monotonicity conditions were satisfied, then the Lax-Wendroff scheme

$$\begin{aligned} f_{k,i,j}^{n+1} &= f_{k,i,j}^n - \frac{c}{2}(f_{k+1,i,j}^n - f_{k-1,i,j}^n) \\ &+ \frac{c^2}{2}(f_{k+1,i,j}^n - 2f_{k,i,j}^n + f_{k-1,i,j}^n), \end{aligned} \quad (27)$$

was applied. Otherwise the upwind scheme

$$f_{k,i,j}^{n+1} = f_{k,i,j}^n - c(f_{k+1,i,j}^n - f_{k,i,j}^n) \quad (28)$$

was used. The sufficient monotonicity conditions are

$$\begin{aligned} 2 |f_{k,i,j}^n - f_{k-1,i,j}^n| &> |f_{k+1,i,j}^n - 2f_{k,i,j}^u| \\ &+ |f_{k-1,i,j}^n|, \quad v_x > 0, \\ 2 |f_{k+1,i,j}^n - f_{k,i,j}^n| &> |f_{k+1,i,j}^n - 2f_{k,i,j}^n| \\ &+ |f_{k-1,i,j}^n|, \quad v_x < 0. \end{aligned}$$

Here $c = \tau v_x / h_x$ is the Courant number, τ is the time step, h_x is the space step, and k , i , and j are indices along the coordinates x , v_x , and v_r , respectively. For $v_x = 0$, the solution remains the same as the initial conditions. Since both schemes are explicit with respect to time, it is necessary to choose the ratio τ/h_x such that the Courant stability condition $\tau|v_x|_{\max}/h_x < 1$ is satisfied. In contrast to the upwind scheme, the Lax-Wendroff scheme is second order, having $O(\tau^2, h_x^2)$ errors, but is not monotone.

Both (27) and (28) applied to the transport stage (24) were tested on the exact stationary solution of the Boltzmann equation (22) with boundary conditions of type (23). In dimensionless variables this solution has the form

$$f_0(x, v_x, v_r) = \begin{cases} f\left(\frac{1}{2}, v_x, v_r\right), & v_x < 0, \\ f\left(-\frac{1}{2}, v_x, v_r\right), & v_x > 0, \\ \frac{1}{2} [f\left(\frac{1}{2}, v_x, v_r\right) + f\left(-\frac{1}{2}, v_x, v_r\right)], & v_x = 0, \end{cases} \quad (29)$$

where

$$\begin{aligned} f\left(\frac{1}{2}, v_x, v_r\right) &= \frac{2\nu}{1+\nu} (2\pi T_+)^{-\frac{3}{2}} e^{-\frac{(v_x^2+v_r^2)}{2T_+}}, \quad v_x < 0, \\ f\left(-\frac{1}{2}, v_x, v_r\right) &= \frac{2}{1+\nu} (2\pi)^{-\frac{3}{2}} e^{-\frac{(v_x^2+v_r^2)}{2}}, \quad v_x > 0, \end{aligned}$$

and $\nu = n_+/n_-$. The solution (29) corresponds to asymptotic free molecular flow¹, where $\text{Kn} \rightarrow \infty$, and it only depends on the parameter ν . The following relations hold:

$$\begin{aligned} \nu &= \frac{1}{\sqrt{T_+}}, \\ n(x_n) &= \int_{R^3} f(x_n, \mathbf{v}) d\mathbf{v} = \frac{1}{2}(n_+ + n_-) = 1, \\ nU_x &= \int_{R^3} v_x f_0(x_n, \mathbf{v}) d\mathbf{v} = 0, \\ T(x_n) &= \frac{2}{3n(x_n)} \int_{R^3} \mathbf{v}^2 f(x_n, \mathbf{v}) d\mathbf{v} = 2\sqrt{T_+}, \\ q_x(x_n) &= \frac{1}{2} \int_{R^3} v_x \mathbf{v}^2 f(x_n, \mathbf{v}) d\mathbf{v} = -2\sqrt{\frac{2}{\pi}} \frac{(1-\nu)}{\nu^2}. \end{aligned}$$

Parameters used in the tests were $\nu = \frac{1}{2}, 1, 2$, $\tau = 0.01$, $h_x = \frac{1}{12}$, $-8 \leq v_x < 8$, $0 < v_r \leq 8$.

The numbers of sample points for both the v_x and v_r variables were 128. For the chosen parameters, the stability condition of the Lax-Wendroff and upwind schemes is satisfied, i.e., the Courant number is $c = 0.96 < 1$.

Analysis of calculations shows that the Lax-Wendroff and upwind numerical schemes give practically the same sufficiently satisfactory results for the mesh distribution function. The greatest errors in hydrodynamic parameters were obtained for $\nu = 2$. The corresponding values for $t = 1.0$ are presented in Table 1. The errors mostly result from the quadrature formula employed despite it being based on the spline interpolation.

Fourier and Hankel discrete transforms were used for solving the Cauchy problem (25) forward and back. Special attention was paid to the discrete Hankel transform for which standard code is absent. The algorithm proposed in¹⁴ was chosen. Applying the exponential change of variables $k_r = k_0 e^x$, $v_r = v_0 e^{-y}$, the initial Hankel transform

$$g(k_r) = 2\pi \int_0^\infty v_r f(v_r) J_0(2\pi k_r v_r) dv_r \quad (30)$$

is reduced to the convolution type integral

$$\hat{g}(x) = 2\pi \int_{-\infty}^\infty e^{2y} \hat{f}(y) J_0(2\pi k_0 v_0 e^{x-y}) dy \quad (31)$$

which can be effectively computed using the standard FFT numerical procedures¹¹. To precisely calculate the high-energy tail of the distribution function, the interval of the velocity variables was chosen as $-v_{\max} \leq v_x \leq v_{\max}$, $0 < v_r \leq v_{\max}$, with $v_{\max} = 8$. For computing the fast Hankel transform (31) we set $v_0 = v_{\max}$, $k_{r_{\max}} = v_{\max} = v_0$, and $v_{r_{\min}} = k_{r_{\min}} = v_0 e^{-(N_r - 1)h_r}$, where N_r is the number of grid points and $h_r = \ln(v_{\max}/v_{r_{\min}})/(N_r - 1)$.

For the Fourier transform with respect to v_x the following values were used

$$h_{v_x} = \frac{2v_{x_{\max}}}{N_{v_x}},$$

$$k_x \in [-k_{x_{\max}}, k_{x_{\max}}) = \left[-\frac{n_{v_x}}{4v_{x_{\max}}}, \frac{n_{v_x}}{4v_{x_{\max}}} \right).$$

In further calculations the numbers of grid points were $N_{v_x} = 256$ and $N_r = 2048$.

The algorithm for solving problem (25), (26) as a whole was tested with the well-known exact solutions of the space-homogeneous Boltzmann equation. For numerical integration with respect to time, the Runge-Kutta schemes of first, second and fourth orders with

the time step $\tau = 0.05$ were applied. The number of sample points on the variables of integration α , μ in the collision integral (19) (over the unit sphere) were both 16. The integrands were evaluated using two-dimensional spline interpolation.

Most of the tests were made with the Bobylev-Krook-Wu (BKW) solution⁹

$$f(t, \mathbf{v}) = \frac{(2\pi)^{3/2}}{(1-\theta)^{3/2}} e^{-\frac{(2\pi)^2}{2(1-\theta)} v^2} \left[1 + \frac{\theta}{1-\theta} \times \left(\frac{(2\pi)^2}{2(1-\theta)} v^2 - \frac{3}{2} \right) \right], \quad \theta = 0.4e^{-t/6}. \quad (32)$$

Its combined Fourier-Hankel transform has the form

$$\varphi(\mathbf{k}, t) = (1 - 0.2k^2 e^{-t/6}) e^{-\frac{k^2}{2} + 0.2k^2 e^{-t/6}}. \quad (33)$$

It is important that for (33) the collision integral is not zero, but is

$$\hat{Q}(\varphi, \varphi) = \frac{0.04}{6} k^4 e^{\left(0.2e^{-t/6} - \frac{1}{2}\right) k^2 - t/3}. \quad (34)$$

Calculations showed that the second and fourth order schemes took an unreasonable amount of computing time. Thus, for further calculations, the first order Runge-Kutta scheme was chosen. The essential component of the realization of the Runge-Kutta scheme both with respect to the volume of calculations and computational precision is the computing of the collision integral. Therefore the computing procedure for the collision integral was separately tested. Comparison of the results of the calculations with the exact solution in the relative L_∞ -norm of error is presented in Table 2. Similar results were obtained for the Maxwell solution

$$f(\mathbf{v}, t) = \frac{1}{(2\pi)^{3/2}} e^{-\mathbf{v}^2/2}, \quad (35)$$

which is the stationary solution of the problem and has a collision integral equal to zero.

CONSERVATION LAWS AT THE RELAXATION STAGE

For computing the relaxation stage it is very important to minimize errors in the discrete versions of the conservation laws for density, mean velocity (momentum) and temperature (energy). A conservative method for the relaxation stage based on a polynomial correction of the computed distribution function was proposed in³. Since in the present paper the relaxation stage is calculated in the Fourier representation (26), one can use the correction of the Fourier transform $\varphi(k_x, k_r, t)$

Table 1 Comparison between exact and numerical solutions at $t = 1$.

moments	exact	$x = -0.5$	$x = 0.0$	$x = 0.5$
n	1	1.00001	0.999998	1.00001
nU_x	0	1.05133×10^{-3}	1.05025×10^{-3}	1.04382×10^{-3}
T	1	1.00001	1.00001	1
q_x	0.398942	0.398958	0.398957	0.398952

Table 2 Comparison between exact BKW and numerical solution (relative L_∞ -norm of error), $\tau = 0.05$.

	$t = \tau$	$t = 2\tau$	$t = 3\tau$	$t = 4\tau$	$t = 5\tau$
$\ \hat{Q}(\varphi, \varphi) - \hat{Q}(\tilde{\varphi}, \tilde{\varphi})\ _\infty$	4.8×10^{-4}	9.5×10^{-4}	1.4×10^{-3}	1.8×10^{-3}	2.2×10^{-3}
$\ \varphi - \tilde{\varphi}\ _\infty$	2.9×10^{-5}	5.5×10^{-5}	8.1×10^{-5}	1.0×10^{-4}	1.2×10^{-4}
$\ f - \tilde{f}\ _\infty$	1.0×10^{-3}	1.9×10^{-3}	2.7×10^{-3}	3.5×10^{-3}	4.3×10^{-3}

proposed in Ref. 15. In this case it is necessary to reformulate (7)–(9) in terms of the function $\varphi(k_x, k_r, t)$. These relations for density, momentum, and energy are

$$\varphi(x, 0, 0, t) = n(x, t) = C_1(x), \quad (36)$$

$$\nabla \varphi|_{k=0} = -2\pi i \mathbf{e}_x n(x, t) u(x, t) = C_2(x) \mathbf{e}_x, \quad (37)$$

$$\frac{1}{2} \Delta \varphi|_{k=0} = -4\pi^2 \left(\frac{3}{2} nT + \frac{1}{2} n\mathbf{u}^2 \right) = C_3(x). \quad (38)$$

In the one-dimensional case, $\mathbf{u} = (U_x, 0, 0)$.

Applying Runge-Kutta schemes for solving equation (26), the density conservation law (36) holds, but there are no discrete analogues of (37) and (38)⁵. To improve on this shortcoming, an asymptotic solution of the relaxation problem (26) near the zero grid point $k_x = k_r = 0$ was applied. The Taylor series expansion of the function $\varphi(h_x, h_r)$ for small h_x and h_r is

$$\begin{aligned} \varphi(t, h_x, h_r) &= \varphi(t, 0, 0) + \delta \varphi|_{k=0} \\ &\quad + \frac{1}{2} \delta^2 \varphi|_{k=0} + O(k^3), \end{aligned} \quad (39)$$

where h_x and h_r are the spacings along corresponding coordinates of the grid points nearest to zero, and δ and δ^2 are differentials of first and second orders. Using the cylindrical symmetry and (36)–(38), one can obtain

$$\begin{aligned} \varphi(t, h_x, h_r) &= n - 2\pi i n U_x h_x - 2\pi^2 n [(U_x h_x)^2 \\ &\quad + \frac{3}{2} h_r^2 T + T_x (2h_x^2 - h_r^2)] + O(h^3), \end{aligned} \quad (40)$$

where

$$n T_x = 2\pi \int_{-\infty}^{\infty} \int_0^{\infty} \frac{1}{2} c_x^2 f(x, t, v_x, v_r) v_r dv_r dv_x. \quad (41)$$

Substitution of expansion (40) into the space homogeneous Boltzmann equation (25) gives

$$2\dot{T}_x + \frac{n}{Kn} T_x = \frac{n}{2Kn} T \quad (42)$$

which has the general solution

$$T_x(t) = \frac{T}{2} + \left(T_x(0) - \frac{T}{2} \right) e^{-nt/2Kn}. \quad (43)$$

The improved procedure for the discrete conservation laws is the following. Let the computation at time step $p+1$ start from the relaxation stage. At the end of the computations at the previous time step p , the values (36)–(38) are used to obtain values of the grid functions n_m^p , $n_m^p U_{x,m}^p$, T_m^p , and $T_{x,m}^p$. These values are used to improve the values of the distribution function at the grid points $(0, 0)$, $(\pm h_x, 0)$, $(0, h_1)$, and $(\pm h_x, h_1)$. Using (40), one obtains

$$\varphi_m^{p+1}(0, 0) = n_m^p, \quad (44)$$

$$\begin{aligned} \varphi_m^{p+1}(\pm h_x, 0) &= n_m^p - 2\pi i n_m^p U_{x,m}^p (\pm h_x) \\ &\quad - 2\pi^2 n_m^p \left[(U_{x,m}^p h_x)^2 + 2T_{x,m}^{p+1} h_x^2 \right], \end{aligned} \quad (45)$$

$$\varphi_m^{p+1}(0, h_1) = n_m^p - 2\pi^2 n_m^p T_{r,m}^{p+1} h_1^2, \quad (46)$$

From the definition of $T(x, t)$ and (43), we get

$$T_{r,m}^{p+1} = \frac{3}{2} T_m^p - T_{x,m}^{p+1}, \quad (47)$$

$$T_{x,m}^{p+1} = \frac{T_m^p}{2} + \left(T_{x,m}^p - \frac{T_m^p}{2} \right) e^{-\frac{n_m^p \tau}{2Kn}}. \quad (48)$$

For small τ , instead of (48) one can write the asymptotic expansion

$$T_{x,m}^{p+1} = \frac{T_m^p n_m^p \tau}{4Kn} + T_{x,m}^p \left(1 - \frac{n_m^p \tau}{2Kn} \right). \quad (49)$$

The improved discrete conservation laws are expressed through (44)–(48) by means of symmetric finite differences which approximate the differential relations (37) and (38) to $O(h_x^2 + h_r^2)$.

For some one-dimensional problems one has $U_x = 0$. To satisfy this conservation law up to $O(h_x^2)$, it is necessary to make

$$\varphi_m^{p+1}(h_x, 0) = \varphi_m^{p+1}(-h_x, 0). \quad (50)$$

NUMERICAL EXAMPLE

To demonstrate the possibilities of the new method the classical one-dimensional heat transfer problem¹ was calculated. From the computational point of view it is of interest because all numerical methods used in rarefied gas dynamics have been tested on this problem.

The problem is set as follows. Monatomic gas is contained between two parallel plates separated by a distance L (see Fig. 1). The plates have fixed temperatures T_- and T_+ , $T_- \leq T_+$. It is assumed that on the plates complete accommodation of momentum and energy hold: molecules leaving the plates have half-space Maxwellian distributions. In dimensionless variables, the stationary problem has the form of (22) with (23). The parameters of the problem are

$$Kn = \frac{1}{\bar{n}\sigma_0 L \sqrt{kT_- / m}},$$

where \bar{n} is the mean number density, and the ratio of the temperatures which is T_+ in the dimensionless form. In this case using impenetrable conditions of the hard boundary surfaces, the values of the densities n_- and n_+ in (23) are given by

$$\frac{n_-}{(2\pi)^{3/2}} + \int_{-\infty}^0 \int_0^\infty f(-\frac{1}{2}, v_x, v_r) v_x v_r dv_r dv_x = 0, \quad (51)$$

$$\frac{n_+}{(2\pi T_+)^{3/2}} + \int_0^\infty \int_0^\infty f(\frac{1}{2}, v_x, v_r) v_x v_r dv_r dv_x = 0. \quad (52)$$

Here the values of the distribution function f are obtained by solving the transport equation at each time step.

In the calculations we used $Kn = 1, 1/2\sqrt{2}, \frac{1}{4}$, and $1/20\sqrt{2}$, with $T_+ = 4$. Such values of the parameters were considered in many papers studying this problem (see Ref. 16 and references therein). In our calculations the grid parameters coincided with the parameters chosen in the tests. The stationary solution of the problem was obtained by an iterative

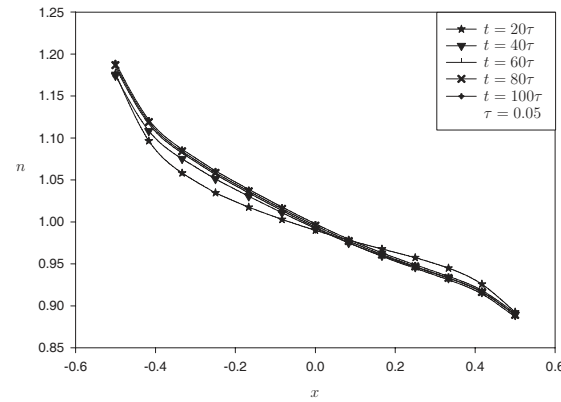


Fig. 2 Convergence of the density profiles for $Kn = \frac{1}{2\sqrt{2}}$.

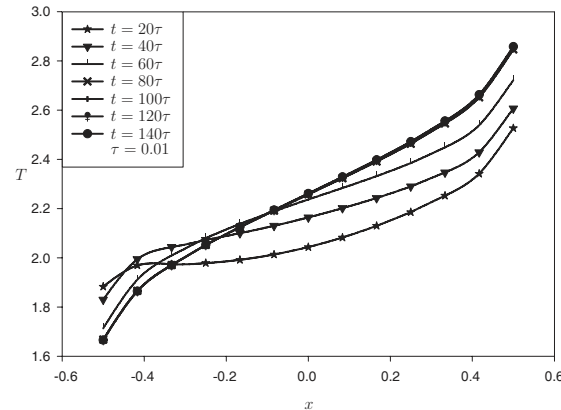


Fig. 3 Convergence of the temperature profiles for $Kn = 1$.

method based on the described splitting method. The time step of the relaxation stage was five times that of the transport stage. In the first set of calculations (with $Kn = 1$) the free molecular solution (29) was used as initial data. In the remaining calculations the results obtained from the previous value of the Kn were taken as the initial data for the smaller Knudsen number.

Convergence of the density profile for $Kn = 1/2\sqrt{2}$ and the temperature profile for $Kn = 1$ are shown in Figs. 2 and 3, respectively. The maximum time values on the graphs correspond to the stationary solutions obtained. Additional control of convergence was carried out through the behaviour of the profiles of the mean velocity U_x and the heat flux q_x . In the stationary solution the mean velocity is $U_x = 0$ and the heat flux is constant. In all calculations these demands were satisfied to an accuracy of $\|U_x\|_\infty \leq 10^{-3}$ and $\|\Delta q_x\|_\infty \leq 0.15$. A relatively large error in the heat flux was obtained at the boundary grid points.

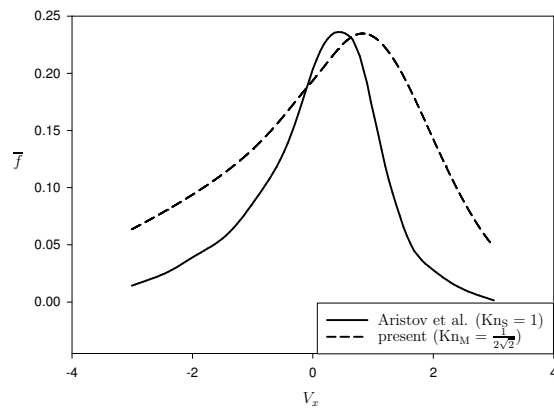


Fig. 4 Comparison of the shearing of the distribution function for $\text{Kn} = 1$.

However, at most other points this error did not exceed 10^{-3} .

There are numerous data for the one-dimensional heat transfer problem with the hard spheres molecular model (see Ref. 16 and references therein). This model is the opposite to the model of Maxwellian molecules with respect to the “rigidity” of molecular collisions. Hence, one can expect satisfactory coincidence neither for the distribution function nor even for the profiles of hydrodynamic variables such as n , T , and q_x . Nevertheless, comparison of corresponding data is useful from the point of view of their qualitative behaviour. Shearing of the distribution function, defined by the relation

$$\bar{f}(x, v_x) = 2\pi \int_0^\infty f(x, v_x, v_r) v_r dv_r,$$

was compared for $x = 0$ as shown in Fig. 4.

Examples of comparison of hydrodynamic parameters are presented in Figs. 5 and 6. Comparisons were made for $\text{Kn}_M = \text{Kn}_S/2\sqrt{2}$, where Kn_M and Kn_S are the Knudsen numbers of the Maxwellian and the hard spheres molecular models, respectively. This relation follows from comparison of the dimensionless forms of the Boltzmann equation for these models.

One can see that in general, the behaviour of the macroscopic parameters and shearing of the distribution function are similar for both models for the Knudsen numbers considered. To explain the differences in the slopes of the hydrodynamic parameter profiles one can derive a corresponding estimation for the density curves. Let us integrate the Boltzmann equation for

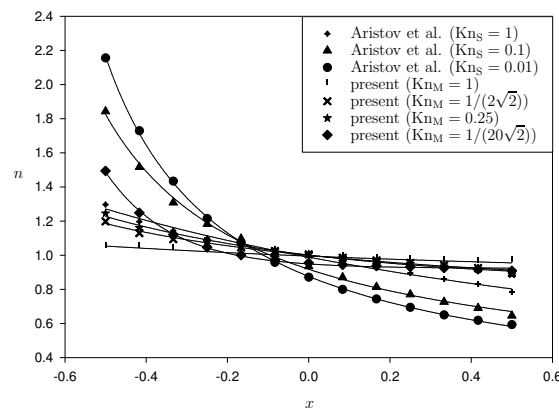


Fig. 5 Density profiles for different Knudsen numbers.

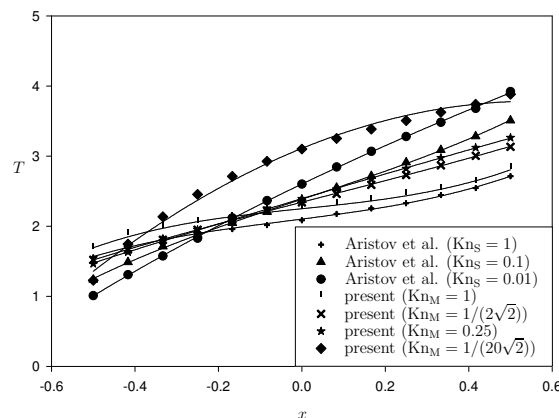


Fig. 6 Temperature profiles for various Knudsen numbers.

the Maxwellian and hard spheres molecular models:

$$\begin{aligned} \left(\frac{dn}{dx} \right)_i &= \frac{d}{dx} \left(\int_{R^3} f(x, \mathbf{v}) d\mathbf{v} \right) \\ &= \int_{R^3} \frac{1}{v_x} c_i Q_i(f, f) d\mathbf{v}, \end{aligned} \quad (53)$$

where $i = 1$ and $i = 2$ correspond to Maxwellian and hard spheres molecules, respectively,

$$\begin{aligned} Q_1 &= \int_{R^3} \int_{S^2} [f' f'_1 - f f_1] d\mathbf{n} d\mathbf{v}_1, \\ Q_2 &= \int_{R^3} \int_{S^2} |\mathbf{v} - \mathbf{v}_1| [f' f'_1 - f f_1] d\mathbf{n} d\mathbf{v}_1, \end{aligned}$$

and $c_1 = (4\pi \text{Kn}_1)^{-1}$, $c_2 = (\sqrt{2}\pi \text{Kn}_2)^{-1}$. For the comparison it was assumed that $c_1 = c_2$. Using the generalized mean value theorem, one can rewrite (53)

as

$$\left(\frac{dn}{dx} \right)_1 = S_1 \times I_1, \quad \left(\frac{dn}{dx} \right)_2 = S_2 \times I_2,$$

where

$$S_1 = \left[\frac{1}{v_x} \frac{[f' f'_1 - f f_1]}{f_0(\mathbf{v}) f_0(\mathbf{v}_1)} \right]_{\mathbf{v}=\mathbf{v}_*, \mathbf{v}_1=\mathbf{v}_{1*}},$$

$$S_2 = \left[\frac{1}{v_x} \frac{[f' f'_1 - f f_1]}{f_0(\mathbf{v}) f_0(\mathbf{v}_1)} \right]_{\mathbf{v}=\tilde{\mathbf{v}}_*, \tilde{\mathbf{v}}_1=\tilde{\mathbf{v}}_{1*}},$$

$$I_1 = \int_{R^3} \int_{R^3} \int_{S^2} f_0(\mathbf{v}) f_0(\mathbf{v}_1) d\mathbf{n} d\mathbf{v}_1 d\mathbf{v},$$

$$I_2 = \int_{R^3} \int_{R^3} \int_{S^2} f_0(\mathbf{v}) f_0(\mathbf{v}_1) |\mathbf{v} - \mathbf{v}_1| d\mathbf{n} d\mathbf{v}_1 d\mathbf{v}.$$

Since the Boltzmann brackets are normalized by the product of Maxwellian functions it can be shown that $|S_1| \approx |S_2|$ and hence

$$\left| \left(\frac{dn}{dx} \right)_2 \right| \approx \frac{4}{\sqrt{\pi}} \left| \left(\frac{dn}{dx} \right)_1 \right|. \quad (54)$$

This means that in any one-dimensional problem under the same conditions the slope of the number density profile for the hard sphere model is greater than that for Maxwellian molecules. Such behaviour can be seen in Fig. 5.

CONCLUSIONS

A new deterministic numerical method for solving the Boltzmann equation with cylindrical symmetry in velocity space for the Maxwell molecular model was developed. The method is based on the splitting scheme with respect to physical processes. The main feature of the method is the use of the Fast Fourier and Hankel procedures which determine a computational efficiency of the method estimated as $O(N \log_2 N)$. Code realizing the proposed algorithm was worked out. All parts of the code were carefully tested on exact solutions. As a sample application of the proposed method, the classical problem of heat transfer between two parallel plates was calculated for a wide interval of the Knudsen numbers. The results of calculations confirmed a good availability of the created mathematical tools. The developed code can be applied to many other similar problems of the gas kinetic theory, some of which were listed at the beginning of the paper.

Acknowledgements: This work was supported by the Thailand Research Fund RGJ PhD programme (Contract No. PHD/0272/2546). One of the authors (Y.N.G.) was partially supported by the Russian Basic Research Fund

(Project No. 08-01-00116). The authors would like to express their special thanks to E. Schulz for valuable discussions. We would also like to thank the Centre for Computing Services and the School of Mathematics at Suranaree University of Technology for making available high performance computing facilities throughout this work.

REFERENCES

1. Kogan MN (1969) *Rarefied Gas Dynamics*, Plenum Press, New York.
2. Cercignani C (1975) *Theory and Application of the Boltzmann Equation*, Elsevier, New York.
3. Aristov VV (2001) *Direct Methods for Solving the Boltzmann Equation and Study of Nonequilibrium Flows*, Kluwer Academic Press, Dordrecht.
4. Bird GA (1976) *Molecular Gas Dynamics*, Clarendon Press, Oxford.
5. Grigoriev YN, Mikhalkin AN (1983) A spectral method of solving Boltzmann's kinetic equation numerically. *USSR Comp Math Math Phys* **23**, 105–11.
6. Pareschi L, Russo G (2000) Numerical solution of the Boltzmann equation. I. Spectrally accurate approximation of the collision operator. *SIAM J Numer Anal* **37**, 1217–45.
7. Filbet F, Russo G (2003) High order numerical methods for the space non-homogeneous Boltzmann equation. *J Comput Phys* **186**, 457–80.
8. Kolobov VI, Arslanbekov RR, Aristov VV, Frolova AA, Zabelok SA (2007) Unified solver for rarefied and continuum flows with adaptive mesh and algorithm refinement. *J Comput Phys* **223**, 589–608.
9. Bobylev AV (1975) The method of Fourier transform in the theory of the Boltzmann equation for Maxwell molecules. *Dokl Akad Nauk SSSR* **225**, 1041–4.
10. Sneddon IN (1972) *The Use of Integral Transforms*, McGraw-Hill.
11. Brigham EO (1974) *The Fast Fourier Transform*, Prentice-Hall.
12. Drikakis D, Rider W (2005) *High-Resolution Methods for Incompressible and Low-Speed Flows*, Springer, Berlin.
13. Larina IN, Rykov VA (2000) Method for numerical solving the Boltzmann equation with linearized collision integral. *Computing Center of the Russian Academy of Sciences*, 3–26.
14. Siegman AE (1977) Quasi-fast Hankel transform. *Optic Lett* **1**, 13–5.
15. Bobylev AV, Rjasanow S (1997) Difference scheme for the Boltzmann equation based on the fast Fourier transform. *Eur J Mech B* **16**, 293–306.
16. Aristov VV, Ivanov MS, Cheremisin FG (1990) Two methods for solving the problem of heat transfer in a rarefied gas. *USSR Comp Math Math Phys* **30**, 193–5.